Thermal shock behaviour of magnesia–spinel composites

Cemail Aksel[a,*], Brian Rand[b], Frank L. Riley[b], Paul D. Warren[b,1]

[a]*Department of Materials Science and Engineering, Anadolu University, Iki Eylül Campus, Eskisehir 26470, Turkey*
[b]*Department of Materials, School of Process, Environmental and Materials Engineering, University of Leeds, Leeds LS2 9JT, UK*

Abstract

The incorporation of up to 30% of spinel powder of median particle sizes 3, 11 and 22 μm into dense magnesia gives improved resistance to thermal shock as indicated both by the R''' thermal shock resistance parameters calculated from measured mechanical properties, and by a standard quench test. The loss of strength of the composite materials in the quench test matched satisfactorily that predicted by the R''' parameter. The maximum benefit from spinel additions was obtained with spinel of the largest particle size, at a loading of 20%. It is postulated that the pre-formed cracks in the composites, resulting from the thermal expansion mismatch between magnesia and spinel, inhibit the accumulation of strain energy during thermal shock.
© 2003 Elsevier Ltd. All rights reserved.

Keywords: $MgAl_2O_4$; MgO; Microcracks; Spinel; Strength; Thermal shock; Young's modulus; *R*-Parameters

1. Introduction

Magnesium aluminate spinel ($MgAl_2O_4$) is an important alternative to chrome ore as a component of magnesia (MgO) based refractories. Chrome ore has been extensively used over many years in a wide range of magnesite–chrome and chrome–magnesite refractories.[1] However, waste chrome-containing materials present a potential environmental hazard. The insoluble Cr^{3+} in Cr_2O_3 and its mixed oxides in buried refractory materials may be oxidised to the $Cr^{(VI)}$ state as chromates and dichromates, which because they can be water-soluble carry the risk of the leaching of chromium into ground water. $Cr^{(VI)}$ has been associated with allergic skin ulceration and is a carcinogen.[2–4] $MgAl_2O_4$ (referred to hereafter as spinel) has therefore been developed as an alternative component to chrome ore. There are additional advantages, in that magnesia–spinel refractories have better resistance to thermal shock than pure magnesia materials, and their resistance to alkali attack is also good. They have also shown significantly (two to three times) longer service lives than conventional magnesia–chrome materials in cement kilns and steel making vessels.[5–7] Spinel is therefore now widely used as the second phase in a wide range of magnesia–spinel and alumina–spinel refractories, for a large number of applications.[6,7] The improved resistance to thermal shock of magnesia–spinel materials has been linked[8,9] to the large difference in thermal expansion coefficient between MgO ($\sim$13.5 MK^{-1}) and spinel ($\sim$7.6 MK^{-1}).[10,11] During cooling from production temperatures in the region of 1650 °C the thermal expansion mismatch generates large tensile hoop stresses around the spinel particles, causing extensive microcracking, with an associated large decrease in strength and modulus.[12] The microcracked composite materials then appear to suffer less damage during subsequent rapid temperature changes. However, there appear to have been very few systematic examinations of the influence of spinel on the response to thermal shock of these materials, and the basis for the improvements in thermal shock resistance has not been examined in detail. The object of the present study was to identify more clearly the separate effects of spinel particle size, and loading on the response of model magnesia–spinel materials to thermal shock, and to test the value of the calculated thermal shock parameters in predicting thermal shock damage.

---

* Corresponding author. Tel.: +90-222-3350580x6355; fax: +90-222-3239501.

E-mail address: caksel@anadolu.edu.tr (C. Aksel), f.l.riley@leeds.ac.uk (F.L. Riley).

[1] Now at: Pilkington plc., Group Research, Technology Centre, Hall Lane, Lathom, Lancashire L40 5UF, UK.

2. Thermal shock damage

The resistance to sudden transient temperature change, thermal shock, of refractory materials is a subject of considerable practical interest which has been explored in detail over many years.[13] When a material is quenched between a temperature T and a lower temperature T_0, its surface attempts to contract but cannot because of the constraint of the still hot interior, and a tensile stress is created in the surface. In the case of a hypothetical *infinitely fast quench,* in which the possibility of heat conduction within the material is excluded, the surface stress (σ_{ts}) is given by:

$$\sigma_{ts} = E\Delta T\alpha/(1 - v) \tag{1}$$

where E is the elastic modulus, $\Delta T = (T - T_0)$, α is the mean thermal expansion coefficient, and v is the Poisson ratio, associated with the biaxial nature of the stress. This equation defines the maximum stress which can be produced by quenching. In practical cases the efficiency of heat transfer to the surface (h), and the thermal conductivity (k) of the material, have to be taken into account and the stress indicated by Eq. (1) is reduced by a factor ψ, so that now:

$$\sigma_{ts} = \psi E\Delta T\alpha/(1 - v) \tag{2}$$

ψ is a function of time and the Biot modulus $\beta = ah/k$, where a is a specimen dimension.

Related thermal shock resistance factors (R) expressing the ability of a material to resist these thermal stresses, are defined in terms of these mechanical and physical properties. In the simplest case of stress arising from the infinitely fast quench of an infinite slab of material with constant heat transfer coefficient the parameter (R) relates to the instantaneous temperature difference ΔT required to create a stress equal to the strength of the material, when failure would be expected to occur. That is:

$$R = \sigma_f(1 - v)/E\alpha \tag{3}$$

In materials containing microcracks arising from thermal expansion mismatch, such as those examined here, interactions involving the microcracks effects are an additional important factor influencing resistance to thermal stress.[14] An established view, supported by experimental evidence from BeO–SiC and MgO–W composites containing three-dimensional crack networks,[15] and single phase magnesium dititanate and β-eucryptite materials with internal thermal expansion coefficient anisotropy[16,17] is that microcracking is beneficial. This is attributed primarily to the fact that the microcrack networks permit accommodation of thermal strain and reduce the thermal stresses; elastic moduli are reduced, and strain to failure is increased. On thermal shocking these materials tend to undergo stable, slower, crack propagation, with progressive further loss of strength.[18]

The response of a material to thermal shock can be assessed experimentally using two broad types of approach. The first, with a basis in thermoelastic theory, uses quenching from high temperature, and measurement of the (critical) temperature change required to cause severe mechanical damage (or complete failure). This test is considered to provide a measure of the stress conditions required to initiate fracture: following crack initiation, crack propagation is assumed to be unstable, fast, and complete. The second approach uses a form of thermal cycling and measures the number of cycles needed to cause a defined extent of mechanical damage. This has as basis an energy balance, involving the energy required for the stable propagation of a pre-existing crack. Values of retained strength and modulus then provide convenient indications of the extent of thermal shock damage.

These two approaches to thermal shock have been treated theoretically in detail.[19,20] In a previously undamaged material the condition for failure during a thermal shock is obtained by setting the maximum permitted thermally induced stress equal to the tensile or bend strength. The set of thermal shock resistance parameters, R, R' and R'', expresses the conditions for failure by crack initiation. For the case of an infinite slab symmetrically heated or cooled with a constant heat transfer coefficient, R' and R'' are defined as:

$$R' = \sigma_f(1 - v)k/E\alpha \tag{4}$$

$$R'' = \sigma_f(1 - v)A/E\alpha \tag{5}$$

where σ_f is the tensile strength, E is the Young modulus, α the mean thermal expansion coefficient, v the Poisson ratio, and k thermal conductivity. Because the stress distributions in bend are similar to those occurring as a result of temperature gradients, bend strength values are often considered to be satisfactory (and more easily obtained). A is a stress reduction term, which is a function of the Biot modulus β ($= ah/k$ where a is the radius or half-width of the specimen and h is the heat-transfer coefficient between the body and the quenching specimen). The parameter R is applicable in the case of instantaneous change in surface temperature with an infinitely large heat-transfer coefficient, when $A = 1$: R defines the minimum temperature difference to produce fracture. R' is applicable for conditions of slow heat transfer when the Biot modulus is small; R'' is applicable in the case where the heating or cooling rate is constant. The maximum resistance to fracture initiation is obtained with high strength and thermal conductivity, and low thermal expansivity and Young modulus. However, avoiding fracture by simply increasing strength can be undesirable because the stored energy can then become very large: crack propagation, once initiated, can be fast and explosive. Under the experimental conditions

of the present work, using an oil bath quench, the appropriate parameter is R.

A second set of parameters (R''' and R'''') is applicable to the case of severe thermal environments, where thermal stress fracture cannot be avoided and the major requirement is to minimize the extent of crack propagation. When the thermal stress propagates a pre-existing crack, the maximum surface area (S_{max}) of the new fracture face is given by:

$$S_{max} \leqslant U/\gamma_{WOF} \qquad (6)$$

where U is the stored elastic energy at fracture and γ_{WOF} is the effective surface energy, or work of fracture per unit projected area of fracture face. A crack will continue to propagate as long as the elastic energy released from the stress field surrounding the crack is greater than the fracture surface energy. The requirement now is to minimise U, which is proportional to $\sigma^2(1-v)/E$. Parameters R''' and R'''' are defined as:

$$R''' = E/\left\{\sigma^2(1-v)\right\} \qquad (7)$$

$$R'''' = E\gamma_{WOF}/\left\{\sigma^2(1-v)\right\} \qquad (8)$$

These are thus related to the ability of the cracked material to resist crack propagation (and further damage). R''' expresses the degree of thermal shock damage in materials with similar crack propagation properties, that is, similar values of γ_{WOF}, R'''' would be applicable to materials with widely differing values of γ_{WOF}, and showing marked differences in brittle-ductile behaviour. To minimize thermal shock damage, large values of the Young modulus and surface energy, and low strength are now required, in contrast to the case for the first set of parameters. However, for practical materials it is clear that R''' and R'''' can not be maximised by letting the strength approach zero. Direct observations of crack development using dye-penetrant, coupled with enhancement by fluorescence, often provide useful complementary information in cases where failure is not catastrophic.

In the work described here on a set of dense magnesia–spinel composites of systematically varied spinel particle size and loading, the usefulness of the R and R''' parameters has been assessed for prediction of behaviour under thermal shock. Parameters were calculated from measured mechanical property values, and compared with the retained strengths and Young moduli after a series of quenches into oil from temperatures up to 1000 °C.

3. Experimental

Spinel grit (MR66, Alcoa, UK); 99.5% purity) was milled and air-classified (Alpine Zig-zag classifier, Augsburg, Germany), to give three batches of powder of median particle sizes $\sim$3, $\sim$11 and $\sim$22 μm. Magnesium oxide powder ("Light" GPR, 99% purity, $\sim$30 nm, BDH, Poole UK), was calcined at 1300 °C for 2 h to yield a 0.5 μm powder of improved compactibility and densification behaviour. Starting powders were blended as isopropanol suspensions by mechanical stirring for 20 min. The isopropanol was removed intitially at 100 °C, and the powder was then dried overnight at 300 °C. The set of dense magnesia-spinel composites containing 5–30% by volume of spinel powder was prepared by hot-pressing mixed powders at 1700 °C and 20 MPa, giving discs 25 mm diameter and approximately 5 mm thick. Flat surfaces were ground with progressively finer silicon carbide powders, to 1000 mesh. Bars were cut of dimension $\sim$25×3×3 mm³, and tensile surfaces were polished to 1 μm diamond. Bend strength and work of fracture values were measured using the standard methods reported earlier.[12] Young moduli were calculated from the load–deflection curves and thermal expansivities were calculated using the rule of mixtures.

Thermal-shock was carried out using a standard quench procedure. Bars were suspended using wire in a vertical tube furnace which was heated to temperatures in the range 200 to 1000 °C. At least 20 min was allowed for thermal equilibration at the selected temperature, and the wire was then cut to allow the bar to drop into a large container of magnetically stirred silicone oil at room temperature (20 °C). The quench temperature (T_q) value used (units °C) in the following discussion is the furnace set point temperature. Bars were cleaned with acetone, dried in an oven at 110 °C, and broken in 3-point bend at a loading rate of 1 mm min^{-1}. Surface cracks in polished materials, and in the surfaces of bars subsequently cross-sectioned, were high-lighted using a dye-penetrant (Zyglo, Magnaflux Ltd., UK), painted on to the surface, and examined under an optical microscope. Fracture faces were examined by scanning electron microscopy (SEM).

4. Results and discussion

Strength, modulus and fracture toughness values for pure hot-pressed MgO and the MgO–spinel composites have been reported,[12] and data for strength and modulus are summarised in Figs. 1 and 2. SEM examination showed that the composites were extensively microcracked: cracks were predominantly intergranular, and it was noted that in many cases the cracking might be better described as grain boundary separation. Indeed, as Fig. 3 shows, the larger spinel particles appear to have a major function of providing the connectivity between MgO grains. Microcrack generation was attributed to the large difference in thermal expansion

coefficient between MgO and spinel ($\sim$13.5 and $\sim$7.6 MK^{-1}), coupled with a strong tendency for small spinel crystals to be precipitated at MgO–MgO grain boundaries. The factors controlling thermal stress resistance, as expressed by the R and R' parameters, of microcracked ceramics have been analysed in some detail[14] and for cases where crack interactions can be ignored a quantitative analysis is possible. However, at high crack concentrations where the distance between cracks is of the order of the crack dimension, crack interaction effects are likely to become important and a full analysis of their influence on modulus and strength is more problematic. In the magnesia–spinel composites examined in this work the typical distance between the (primarily grain boundary) cracks is of the order of the crack length and approximately the MgO grain dimension: the effects on elastic behaviour of possible crack interaction effects are therefore more difficult to quantify. In many materials containing high densities of microcracks the effect of microcracking appears to be greater on modulus, than on strength, and the strength/modulus ratio is increased compared to that for the uncracked

material, with consequent increases in R and R'.[21] However, in the present set of materials the strength/ modulus ratio was always smaller than that for the pure MgO (Fig. 4). The reason for this is assumed to be the nature and location of the microcracks in the composites, which for the most part corresponded to the MgO–MgO grain boundaries. Their influence on strength, for a given crack density, might therefore be expected to be much greater than for randomly oriented and located cracks. Fracture in the composites predominantly followed these grain boundaries.

The calculated R parameters for pure MgO and the composites are shown in Fig. 5. It is clear that an assumption that the thermal shock behaviour of the composites can be described by a simple crack initiation
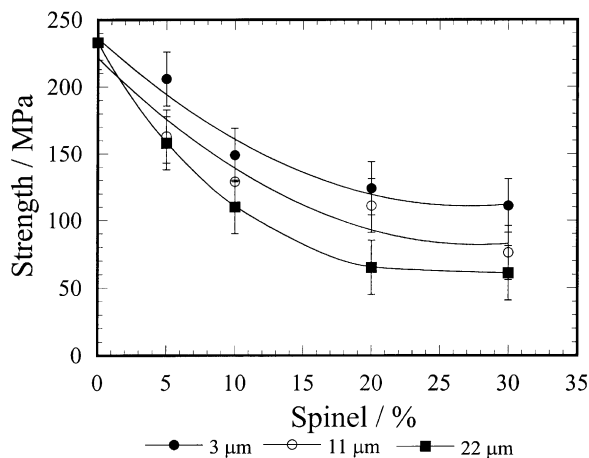

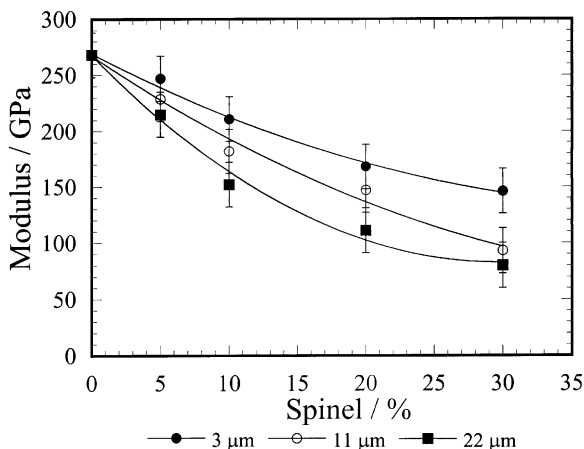Fig. 1. Strength of pure MgO and MgO–spinel composites.

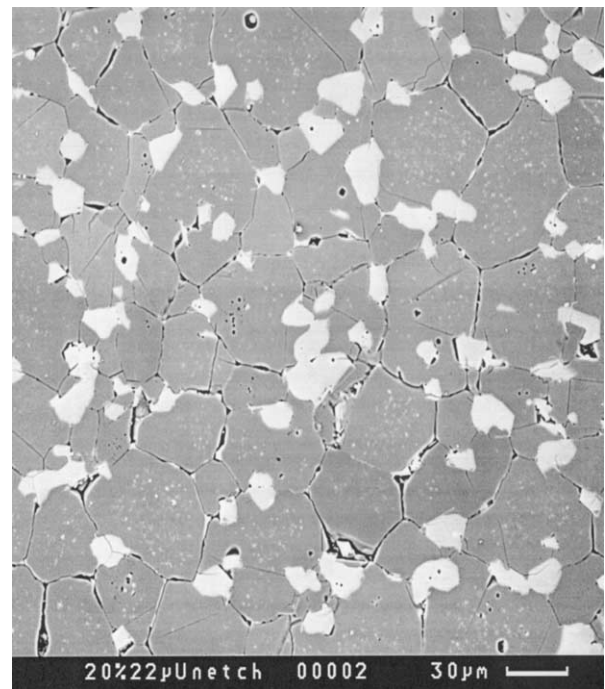Fig. 2. Young modulus of pure MgO and MgO–spinel composites.

Fig. 3. SEM of polished face of a 20%, 22 μm spinel composite, showing extensive grain boundary microcracking.
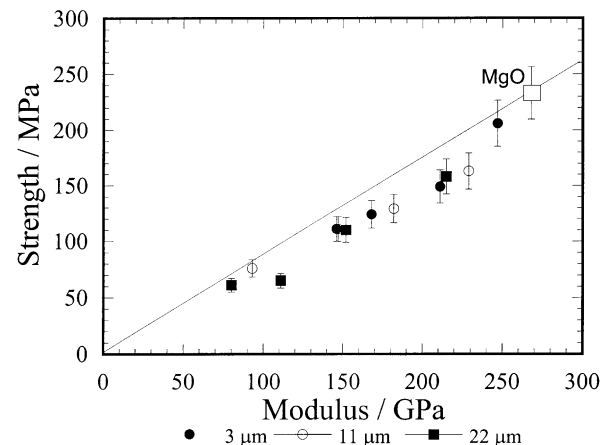

Fig. 4. Strength and modulus values as a function of composition.

and rapid failure model does not predict the improvements in thermal shock behaviour seen with commercial refractories of this type. This is perhaps not surprising, because the applicability of the concept of crack initiation followed by instantaneous failure is not so obvious for materials which already contain a very high density of microcracks: in the weakened and less rigid composites it is unlikely that sufficient strain energy can be generated to cause catastrophic failure. It is more reasonable to view the system from the standpoint of the enhancement of damage by stable, slow, crack propagation; and the R''' parameters shown in Fig. 6 indicate that there should be reduced thermal shock damage compared with that in pure MgO. The R''' parameters increase steadily with increasing spinel loading, and the largest spinel particles have the greatest effect. The best material in this set would be that containing 20% of 22 µm spinel: the indication is that, broadly, the effect is directly proportional to spinel loading, and the larger the spinel particles, the better.
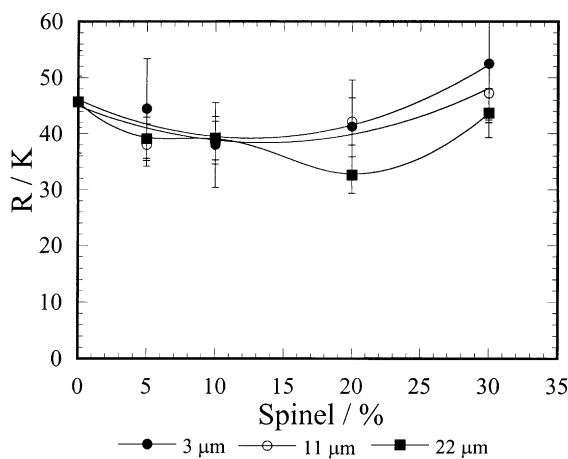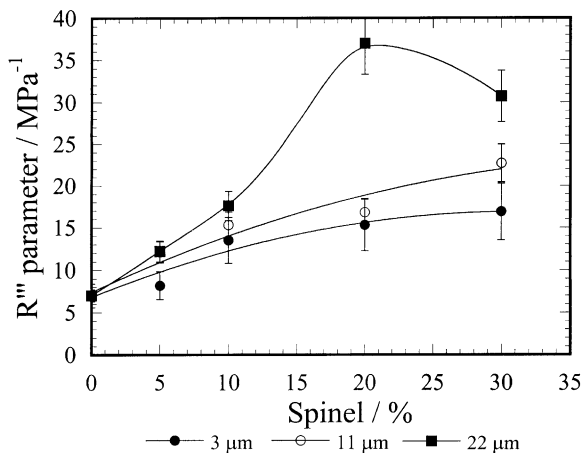
Because the overall differences in elastic behaviour and failure mechanisms of the composites are not great it would not be expected that the work of fracture (incorporated in the R'''' parameter) would make a significant difference to the ranking. γ_{WOF} values are shown in Fig. 7. While there is an approximately 50% increase from that of the pure MgO (from 40 to 60–80 J m^{-2}), the values are not sensitive to loading or spinel particle size. For this reason the R'''' parameter plot follows the same pattern as that of R''' (Fig. 8), and the ranking is unaltered.

The influence of quench temperature on strength is shown in Fig. 9. The effect on modulus was similar. Pure MgO behaves as would be expected for a strong material. Strength is unchanged up to a critical quench temperature (T_{qc}) of ∼600 °C when there is an abrupt loss of strength to about 20% of the initial value. In contrast the weaker composites simply steadily lose strength with increasing quench temperature, with the stronger members of the set being the most influenced.
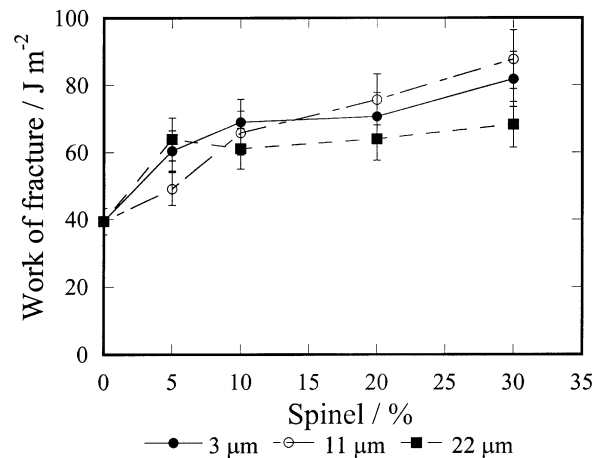

Fig. 5. Calculated R parameters for pure MgO and MgO–spinel composites.

Fig. 7. γ_{WOF} as a function of composition.

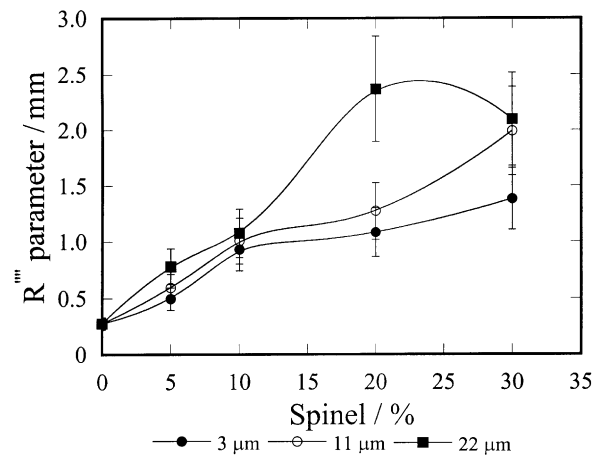Fig. 6. Calculated R''' parameters for pure MgO and MgO–spinel composites.

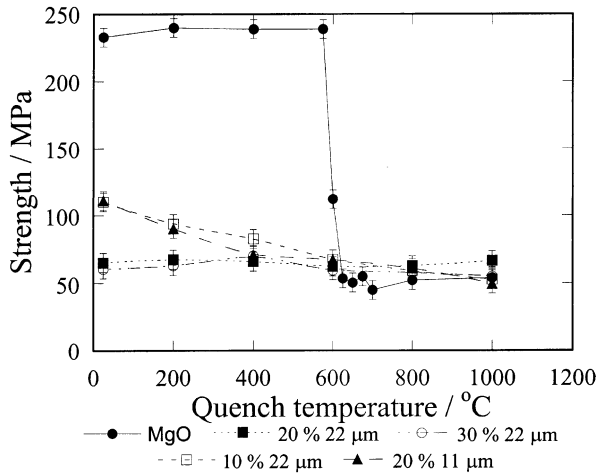Fig. 8. Calculated R'''' parameters for pure MgO and MgO–spinel composites.

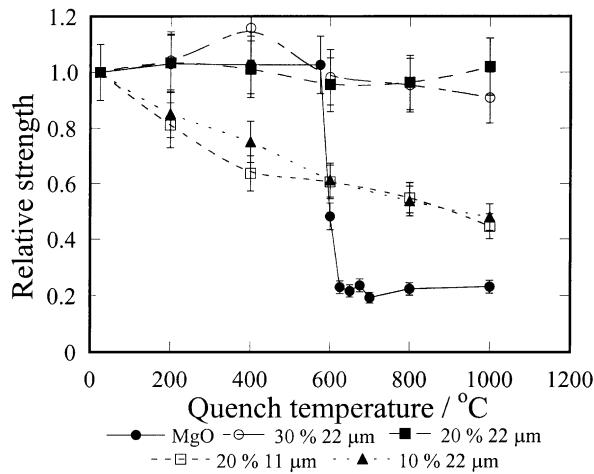Fig. 9. The influence of quench temperature (T_q) on strength.

Fig. 10. Fraction of strength retained as a function of T_q.

Fig. 11. Fraction of strength retained after quenching from 800 °C as a function of R''' parameter.

These data are shown more clearly in Fig. 10, in which fraction of strength retained is plotted as a function of T_q. Young Modulus values again follow the same pattern, though there is a slight loss in stiffness in pure MgO below the critical quench temperature. This suggests that while some damage may be being induced by even weak thermal shocks, the crack size remains below that of the critical value for this material, which has been associated with the grain size.[22]

The quality of the agreement between the predictions of the calculated R values and the actual thermal shock behaviour can readily be determined by comparing the parameter with a quantitative measure of thermal shock damage.[23] Here we use the fraction of strength retained after a quench from 800 °C as indicator, and the plot is shown in Fig. 11. The relationship is good, and indicates that the minimum R''' value for 95% strength retention after quenching from 800 °C is ∼30 MPa^{-1}. This corresponds to a minimum spinel particle size of ∼22 μm, and a minimum loading of ∼20%. From the

point of view of unshocked strength, and thus absolute performance, this is the best material in this set.

Fracture surfaces of bars of pure MgO quenched from temperatures < 575 °C showed a high proportion of transgranular cracks formed by grain cleavage. Low magnification observations aided by the use of dye-penetrant on polished faces, and cross-sections through the centres of bars quenched from temperatures up to 575 °C showed no large scale cracking. At a T_q of 575 °C there was a small increase in the proportion of intergranular fracture, and at the critical quench temperature of 625 °C there was a marked change in the appearance of the fracture surface, which now contained a high proportion of facetted grains produced by intergranular cracking. The polished faces showed a large number of cracks, with a small number progressing towards the bar centre. With quenches from above T_{qc} major cracks became visible on polished surfaces and at the centres of bar on cross-sections

The composites had no specific quench temperature at which a sudden increase in major crack density occurred. There were no detectable major cracks in the 20% 22 μm composite for T_q < 600 °C, but above T_q 600 °C crack density increased with increasing T_q. But even at this T_q new cracks appeared not to have extended to the bar centres: the distance of crack penetration remained small, consistent with the small reductions seen in strength. Fracture surfaces of the 20% 22 μm spinel composite quenched from between 200 and 1000 °C showed no changes in fracture type, which was always predominantly intergranular.

5. Conclusions

The critical quench temperature into silicone oil for pure dense MgO is ∼600 °C: above this temperature strength and Young modulus fall abruptly to 20% of the as-sintered values. The already microcrack weakened

MgO–spinel composites progressively lose strength and modulus with increasing quench temperature: there is no critical quench temperature. The composites have a much higher proportion of retained strength after thermal shock than pure MgO irrespective of composition. Composites formed with coarse spinel particles have better resistance to thermal shock damage than those formed with fine particles. There is a general trend for the thermal shock characteristics to improve with increased loading of spinel, but there is no real advantage in using additions of > 30%: in this set of materials the smallest relative loss of strength on quenching was obtained by the addition of 20% of 22 μm spinel.

The R (crack initiation) parameter fails to predict the observed losses of mechanical integrity in the composites after thermal shock: instead, there is a closely linear relationship between the changes in strength and the R''' (crack propagation) parameter. The improved resistance to thermal shock damage of the microcracked MgO–spinel composites is attributed to the increased difficulty of developing the strain energy required to propagate the thermal expansion mismatch microcracks, because of the extensive grain boundary thermal expansion mismatch microcracking.

Acknowledgements

References

1. Moore, B., Frith, M. and Evans, D., Developments in refractories for cement kilns. *World Cement*, 1991, 5–12.
2. Tabbert, W. and Klischat, H. J., Magnesia-spinel bricks for the cement industry. In *Proceedings of 2nd International Symposium on Refactories*, ed. X. Zhong, J. Lu, X. Yan and M. Li. International Academy Publishers, Beijing, 1992, pp. 424–430.
3. Kuennecke, M., Wieland, K. and Faizullah, M., The correlation between burning zone linings and operation of cement rotary kilns. *World Cement*, 1986, **Part 2**, 247–253.
4. Bartha, P., Magnesia spinel bricks—properties, production and use. In *Proc. Int. Symp. Refractories, Refractory Raw Materials and High Performance Refractory Products*, ed. X. Zhong et al. Pergamon, Hangzhou, 1989, pp. 661–674.
5. Reyes Sanchez, J. A. and Toledo, O. D., New Developments of magnesite–chrome brick and magnesite–spinel for cement rotary kilns—higher thermal shock resistance and higher coating adherence. In *UNITECR '89 CONGRESS,* Anaheim, USA, 1989, pp. 968–979.
6. Dal Maschio, R., Fabbri, B. and Fiori, C., Industrial applications of refractories containing magnesium aluminate spinel. *Industrial Ceramics*, 1988, **8**(3), 121–126.
7. Gonsalves, G. E., Duarte, A. K. and Brant, P. O. R. C., Magnesia–spinel brick for cement rotary kilns. *Am. Ceram. Soc. Bull.*, 1993, **72**(2), 49–54.
8. Wilson, D. R., Evans, R. M., Wadsworth, I. and Cawley, J., Properties and applications of sintered magnesia alumina spinels. In *UNITECR '93 CONGRESS,* Sao Paulo, Brazil, 1993, pp. 749–760.
9. Kimura, M., Yasuda, Y., and Nishio, H., Development of magnesia–spinel bricks for rotary cement kilns in Japan. In *Proc. 26th Int. Col. Ref*, Interceram Special Issue, 1984, 33, Aachen, Germany, 1983, pp. 344–76.
10. Shackelford, J. F., Alexander, W., Park, J. S. et al., ed., *CRC Materials Science and Engineering Handbook*. CRC Press, Boca Raton, FL, 1994.
11. Burnett, S. J., *Properties of Refractory Materials*. UKAEA Research Group Report. Harwell, 1969.
12. Aksel, C., Rand, B., Riley, F. L. and Warren, P. D., Mechanical properties of magnesia–spinel composites. *J. Eur. Ceram. Soc.*, 2002, **22**(5), 745–754.
13. Kingery, W. D., Factors affecting thermal stress resistance of ceramic materials. *J. Am. Ceram. Soc.*, 1955, **38**(1), 3–15.
14. Hasselman, D. P. H. and Singh, J. P., Analysis of thermal stress resistance of microcracked brittle materials. *Am. Ceram. Soc. Bull.*, 1979, **58**(9), 856–860.
15. Rossi, R. C., Thermal-shock-resistant ceramic composites. *Am. Ceram. Soc. Bull.*, 1969, **48**(7), 736–737.
16. Bush, E. A. and Hummel, F. A., High temperature mechanical properties of ceramic materials—I. *J. Am. Ceram. Soc.*, 1958, **41**(6), 189–195.
17. Bush, E. A. and Hummel, F. A., High temperature mechanical properties of ceramic materials—II. *J. Am. Ceram. Soc.*, 1959, **42**(8), 388–391.
18. Hasselman, D. P. H., Unified theory of thermal shock fracture initiation and crack propagation in brittle ceramics. *J. Am. Ceram. Soc.*, 1969, **52**(11), 600–604.
19. Hasselman, D. P. H., Elastic energy at failure and surface energy as design criteria for thermal shock. *J. Am. Ceram. Soc.*, 1963, **46**(11), 535–540.
20. Hasselman, D. P. H., Thermal stress resistance parameters for brittle refractory ceramics: a compendium. *Am. Ceram. Soc. Bull.*, 1970, **49**(12), 1033–1037.
21. Hasselman, D. P. H., Analysis of the strain at fracture of brittle solids with high densities of microcracks. *J. Am. Ceram. Soc.*, 1969, **52**(8), 458–459.
22. Itoh, A., Itatani, K., Howell, F. S., Kishioka, A. and Kinoshita, M., Sintering of magnesium oxide powder prepared by vapour-phase oxidation process—relationships between particle size and mechanical properties of consolidated specimens. *J. Mater. Sci.*, 1996, **31**, 305–317.
23. Cuppola, J. A. and Bradt, R. C., Thermal shock damage in SiC. *J. Am. Ceram. Soc.*, 1973, **56**(4), 214–217.